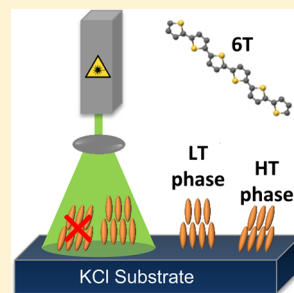


Light Controls Polymorphism in Thin Films of Sexithiophene

Linus Pithan,[†] Caterina Cocchi,^{†,‡} Hannes Zschiesche,[†] Christopher Weber,[†] Anton Zykov,[†] Sebastian Bommel,^{†,§} Steven J. Leake,^{||,#} Peter Schäfer,[†] Claudia Draxl,^{†,‡} and Stefan Kowarik^{*,†}[†]Institut für Physik, Humboldt-Universität zu Berlin, Newtonstr. 15, 12489 Berlin, Germany[‡]IRIS Adlershof, Humboldt-Universität zu Berlin, Zum Großen Windkanal 6, 12489 Berlin, Germany[§]Deutsches Elektronen-Synchrotron (DESY), Notkestr. 6, 22607 Hamburg, Germany^{||}Swiss Light Source, Paul Scherrer Institut, 5232 Villigen PSI, Switzerland

Supporting Information

ABSTRACT: We investigate the influence of light on the growth process and resulting phase coexistence of the organic semiconductor α -sexithiophene (6T). We demonstrate that 6T thin films deposited on potassium chloride (KCl) in dark environments exhibit a bimodal growth, with phase coexistence of both low-temperature (LT) and high-temperature (HT) polymorphs. In contrast, films grown under illumination with 532 nm light at 1.5 W/cm² exhibit an increased purity of the LT phase, while the HT phase growth is slowed down by about a factor of 4. To understand the mechanism behind this optical control, we use in situ X-ray diffraction, atomic force microscopy, optical absorption measurements, as well as first-principles calculations for the optical absorption spectra of the HT and LT phase. We deduce that the phase purification is due to optical heating of the molecular film and lower cohesive energy of the HT phase compared to the LT phase, so that nucleation and growth of the HT phase are significantly reduced by light. On the basis of these findings, we suggest using light as a control parameter in organic molecular beam deposition to grow thin films of enhanced phase purity.



INTRODUCTION

The ability to control crystallization in organic thin films has recently been addressed as one of the current challenges for high-performance organic devices.¹ Since molecular packing and thin film morphology are crucial for the electrical performance of devices such as transistors,² there is an ongoing need to find ways to influence the structural parameters of organic thin films. In many cases the presence of two or more phases in organic films creates structural defects or disorder, thereby impeding charge transport.³ Several strategies to access different growth regimes and to influence the crystal structure, such as changing substrate temperature, evaporation rate, or supersonic thin film growth,⁴ have been pursued. It has also been shown that molecular and substrate symmetries as well as surface corrugations strongly influence the crystalline structure.^{5,6}

A particularly simple control parameter for molecular growth is light, because it does not interfere with the growth environment. Moreover, it can be applied locally and in a controlled way. It is known that some organic molecules polymerize under photoexcitation, and thereby the molecular building blocks are changed, e.g., in C₆₀ films⁷ under intense illumination of 20 W/cm² or in monolayers of sexithiophene under strong UV irradiation.⁸ The electronic properties, such as the surface potential, can also be changed through illumination during growth, as shown by Sugi et al.⁹ The morphology of thin films can be altered as demonstrated by Balzer and Rubahn,¹⁰ who showed that laser illumination leads to a local formation of nanostructures due to increased substrate temperature or

photoinduced electrical charging, as presented by Chen et al. for pentacene monolayers.¹¹ Furthermore, it has been shown that molecules can align with respect to the polarization direction of light when illuminated during growth.¹² In conclusion, there is a high potential for light as a control parameter in organic thin film growth through a variety of interaction mechanisms. However, so far, no direct influence of light on the molecular crystal structure has been reported.

α -Sexithiophene (6T) is a well-studied organic semiconductor often used in thin film transistors¹³ as well as in organic photovoltaics.^{14,15} 6T thin films are crystalline but exhibit bimodal growth of both low-temperature¹⁶ (LT) and high-temperature¹⁷ (HT) phases (see Figure 1a). Both phases also occur in single crystals when grown from melt (HT-phase)¹⁸ or by sublimation (LT-phase).¹³ For thin films of 6T and the structurally similar quaterthiophene (4T), a number of studies report on the occurrence of the HT-phase as well as further crystal polymorphs.^{4,19–24} In 6T bulk crystals the HT-phase is predicted to be more stable than the LT phase.²⁵ The tilt angle ϕ of the long molecular axis and the small basal plane of the unit cell varies for the two structures $\phi_{LT} = 65.9^\circ$ and $\phi_{HT} = 56.3^\circ$.²⁶ This different molecular tilt angle results in a different lattice spacing of 22.35 Å for the LT and 20.67 Å for the HT phase in the direction normal to the substrate surface (Figure 1a).¹³ Thin films of 6T grown on potassium chloride

Received: November 28, 2014

Revised: January 21, 2015

Published: January 30, 2015

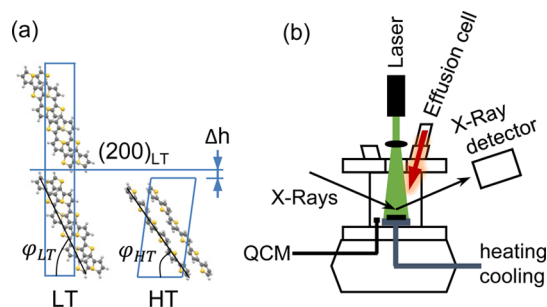


Figure 1. (a) Low-temperature (LT) and high-temperature (HT) phase of 6T. The unit cell of LT (HT) consists of four (two) molecules. The molecular tilt angle ϕ is shown for both structures. (b) Deposition geometry used in the experiment. Compared to conventional organic molecular beam deposition setups a 532 nm laser is added to illuminate the sample during growth.

(KCl) are known to be crystalline, and consist of upright standing and flat lying molecules, where upright standing molecules often nucleate at lying down molecules in so-called ledge directed epitaxy.^{27,28} The different molecular orientations and crystal structures are characterized by specific spectroscopic signatures in UV–vis emission, depending on the intermolecular and molecule–substrate interactions, as shown in refs 29 and 30 for coverages of a few monolayers.

In this paper we show that laser illumination of 6T during growth leads to thin films with higher phase purity compared to those grown in the dark, suggesting that light can be used as a new control parameter to influence the molecular crystal structure in organic thin film growth. We find that illumination during growth suppresses the formation of HT crystallites by about a factor of 4 and increases LT phase purity, thereby improving the quality of the thin film.

EXPERIMENTAL METHODS

We used a portable deposition chamber equipped with a beryllium window for in situ X-ray measurements to grow the samples. We grew 6T films by thermal evaporation in an organic molecular beam deposition (OMBD) vacuum chamber at a base pressure of 7×10^{-7} mbar. A laser beam (continuous wave, 532 nm, 1.5 W/cm^2 on the sample) enters the vacuum chamber perpendicular to the substrate surface (Figure 1b). A telescope expands the laser beam to a full width half-maximum (fwhm) of 14 mm, so that the $10 \times 10 \text{ mm}^2$ substrate is homogeneously illuminated. The cleaved KCl substrates were heated up to $420 \text{ }^\circ\text{C}$ in a vacuum to reduce surface contamination prior to the deposition. All films were grown with molecular deposition rates between 1 and $1.5 \text{ } \text{\AA}/\text{min}$ to a thickness of $(150 \pm 20) \text{ } \text{\AA}$. The film thickness was monitored with a quartz crystal microbalance during growth.

The grown thin films were analyzed by means of X-ray diffraction in a θ - 2θ geometry, in which the out-of-plane scattering vector $q_z = (4\pi/\lambda) \sin \theta$ is varied to study the out-of-plane lattice constant. Laboratory measurements were carried out with a rotating anode X-ray source using Cu– K_α radiation (wavelength $1.54 \text{ } \text{\AA}$). Real time measurements were performed at the surface diffraction end station of the MS beamline at the Swiss Light Source (Paul Scherrer Institute, Switzerland) using a photon counting Pilatus 100k detector.³¹ For these measurements a wavelength of $0.77 \text{ } \text{\AA}$ was used.

The AFM micrographs were recorded with a Bruker Multimode 8 instrument driven in a peak force tapping mode (ScanAsyst). UV/vis absorption data were collected with a Lambda 950 spectrometer (PerkinElmer).

COMPUTATIONAL METHODS

The optical absorption spectra of LT and HT have been computed from first-principles in the framework of density-functional and many-body perturbation theory (MBPT). All calculations have been performed with the exciting code,³² a full-potential, all-electron package, based on the linearized augmented plane wave method. The macroscopic dielectric function has been obtained by solving the Bethe–Salpeter equation (BSE).³³ This represents the most accurate ab initio methodology to describe optical excitations in solids. The electron–hole interaction is explicitly treated, and therefore excitonic effects are quantitatively described. Additional details about the methodology and its implementation in exciting can be found in ref 34. In order to investigate the role of absorption strength in suppressing the HT phase growth upon laser irradiation, we compute the optical absorption spectra for both HT and LT phase as the HT absorption is not accessible experimentally. The characterization of the samples shows that crystalline islands extend for about 500 nm in the lateral direction and roughly 10 monolayers ($\sim 22 \text{ nm}$) in the normal direction with respect to the substrate (for samples grown at $60 \text{ }^\circ\text{C}$ substrate temperature, see Figure 2a). As such, they can be modeled to

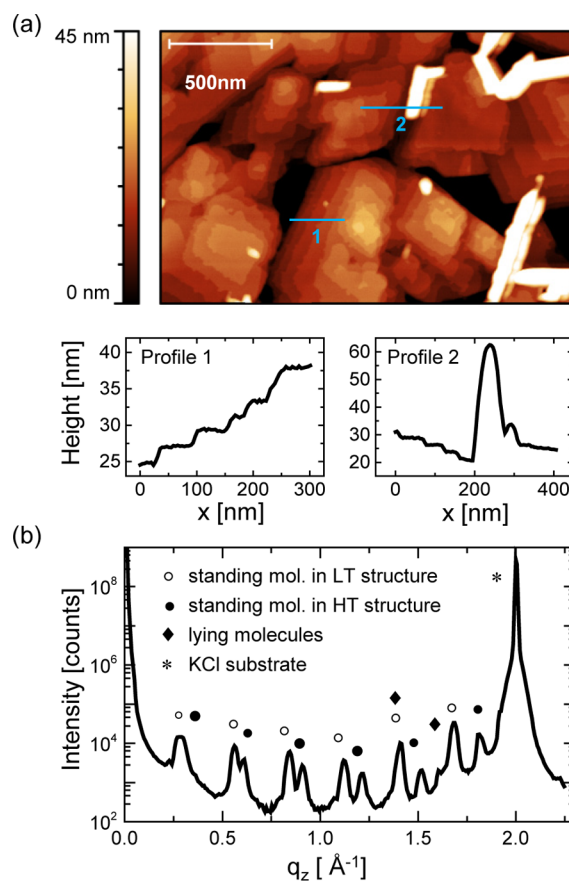


Figure 2. (a) AFM micrograph showing the surface morphology of a 6T film on KCl grown in the dark at $T_{\text{sub}} = 60 \text{ }^\circ\text{C}$. Standing molecules form terraces with monomolecular step height and some “needle-like” structures (white) are formed by flat lying molecules. (b) $\theta/2\theta$ scan of a 6T film as shown in panel a.

good approximation as bulk structures. For computational feasibility, the LT structure has been considered in a reduced unit cell including only two inequivalent molecules. A ground-state calculation within the local-density approximation (LDA)³⁵ for the exchange–correlation potential has been performed, as a starting point for the solution of the BSE. A k-point mesh of $4 \times 6 \times 2$ and $2 \times 4 \times 6$, respectively, has been used for the sampling of the Brillouin zone in the HT and LT phase. One hundred empty states, corresponding to an energy cutoff of about

9 eV above the Fermi energy, have been included to set up the screened Coulomb interaction. Transitions between a set of 20 valence and 20 conduction bands, corresponding to 2.6 eV below the valence band maximum and 2.3 eV above the conduction band minimum, have been taken into account for the solution of the BSE. A rigid shift of 1.37 eV has been applied to the optical spectra of both phases, in order to mimic the quasiparticle correction to the gap.

RESULTS

To get an overview of the postgrowth 6T film morphology, Figure 2a shows an AFM scan of a 150 nm thick 6T film on KCl grown without laser illumination at $T_{\text{sub}} = 60^\circ\text{C}$. Islands of upright standing molecules with terraces of monomolecular step height of (22 ± 2) Å are clearly visible, as well as some “needle-like” structures consisting of flat lying molecules are seen, in agreement with previous AFM results by Schwabegger et al.²⁷ The step height difference between HT and LT phases cannot be resolved in our AFM image because it differs by only 2 Å. A corresponding X-ray $\theta/2\theta$ scan is shown in Figure 2b, exhibiting multiple Bragg reflections due to upright standing molecules. Interestingly, these Bragg reflections are split into pairs, indicating a polymorphous growth behavior of the upright standing molecules in both LT and HT crystal structures. Note that in the LT structure the long unit cell axis is defined as “*a*”, whereas in the HT structure it is “*c*”.^{16–18,36} For the LT structure, the $\{100\}$ plane forms the contact plane with the substrate resulting in $(h00)$ labels for corresponding Bragg reflections, whereas for the HT phase the $\{001\}$ plane forms the contact plane to the substrate resulting in $(00l)$ labels for Bragg reflections of the HT phase. The higher-order Bragg reflections suggest high structural order of the crystalline islands. At higher q_z the (411) and (020) Bragg reflections, which correspond to flat lying molecules, and the (200) KCl substrate reflection, are visible (see Supporting Information for details).

In Figure 3a we compare the Bragg reflections of films grown in the dark and under illumination, with otherwise identical growth conditions. The blue curve corresponds to a film grown at $T_{\text{sub}} = 60^\circ\text{C}$ without illumination, while the red curve corresponds to a sample exposed to 532 nm laser illumination during thin film growth. Interestingly, the HT polymorph is significantly suppressed. In other words, illumination with 532 nm laser light increases the LT phase purity of the thin film. In order to define a quantitative measure for the increased film purity, we use the quantitative phase analysis formalism within the Rietveld method (see Supporting Information).^{37,38} From this we deduce under the given constraints the relation

$$\frac{m_{\text{HT}}}{m_{\text{LT}}} = \frac{I_{(hkl)_{\text{HT}}}}{I_{(hkl)_{\text{LT}}}} \frac{Z_{\text{LT}} V_{\text{LT}}}{Z_{\text{HT}} V_{\text{HT}}} \frac{F_{(hkl)_{\text{HT}}}^2}{F_{(hkl)_{\text{LT}}}^2}$$

with $m_{\text{HT}}/m_{\text{LT}}$ being the mass ratio between two coexisting crystal phases HT and LT in the sample, I the measured reflection intensity, Z the number of 6T molecules per unit cell, and V the respective unit cell volume. We calculated the structure factors, which describe the strength of the Bragg reflections, to be $F_{(600)_{\text{LT}}} = 51.8$ and $F_{(003)_{\text{HT}}} = 24.6$.³⁹ For the films shown in Figure 3a, this leads to a mass ratio of $(m_{\text{HT}}/m_{\text{LT}})_{\text{dark}} = 0.077$ and $(m_{\text{HT}}/m_{\text{LT}})_{\text{illum}} = 0.27$ respectively; thus the growth of the HT phase is suppressed by a factor of 3.5. Using this quantitative measure we consistently find a reduction of the HT phase content by a factor of 3–5 for more than 20 samples grown in this study, with the exact factor depending on

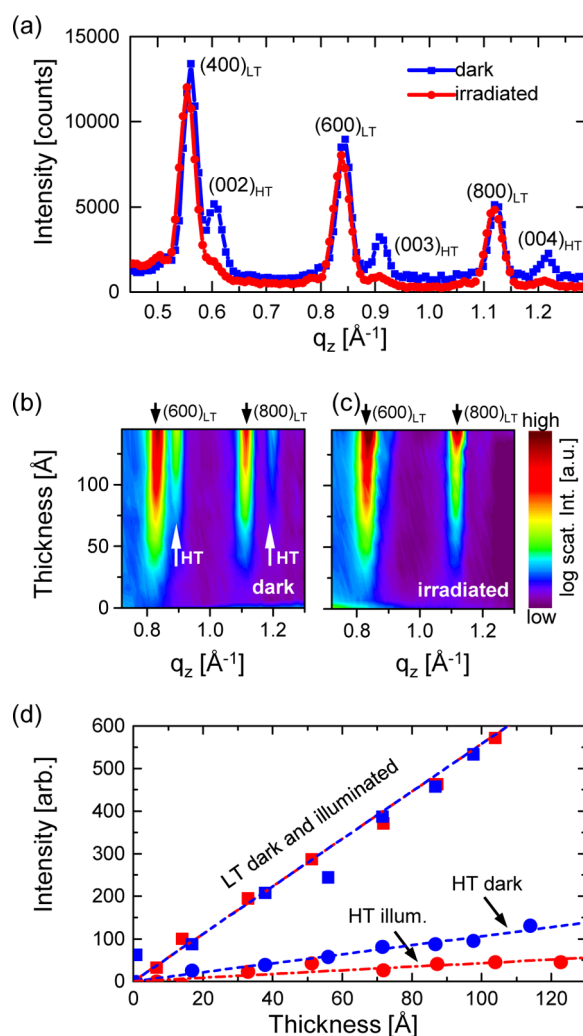


Figure 3. (a) Postgrowth $\theta/2\theta$ scans of 6T films on KCl grown in the dark (blue) and under illumination (red). The time-resolved scattering intensity for the $(600)_{\text{LT}}/(003)_{\text{HT}}$ and $(800)_{\text{LT}}/(004)_{\text{HT}}$ reflection pairs is shown for films grown in (b) the dark and (c) illuminated environment. (d) Square root of the Bragg reflection intensities with and without illumination.

substrate temperature during growth and also on variations in microscopic substrate quality, such as variations in KCl step edge density on cleaved surfaces.

To study the early stage nucleation behavior of HT and LT polymorphs and to find out whether both nucleate simultaneously or one phase appears after a critical thickness, we monitored the thin film growth process by means of time-resolved in situ X-ray measurements during growth. In Figure 3b,c we present the Bragg intensity of the $(600)_{\text{LT}}/(003)_{\text{HT}}$ and $(800)_{\text{LT}}/(004)_{\text{HT}}$ reflections, which increases as a function of film thickness (that is growth time \times molecular flux). Figure 3b shows the thin film growth in a dark environment with fairly strong reflections of the HT structure. In contrast, in the film grown under illumination (Figure 3c) the HT reflections are barely visible. In Figure 3d we present the integrated intensities of the $(600)_{\text{LT}}$ and $(003)_{\text{HT}}$ Bragg reflections, which increase linearly with the thickness of the emerging film. Both with and without laser illumination, at the start, there is no delay in HT phase formation and both phases crystallize simultaneously. However, the growth rate of the HT phase is reduced by a time independent factor via laser illumination.

After demonstrating the impact of laser illumination on phase purity, we show here that this effect is not simply caused by laser-induced heating of the substrate, but by interaction of the laser light with the molecular film. The use of an optically transparent substrate allows us to exclude significant absorption of light in the substrate. We estimate the uncertainty in the substrate temperature measurement at the sample holder to be in the range of ± 5 °C with and without laser illumination. To exclude an influence of this small temperature uncertainty, in Figure 4a we compare films grown in a range of 60 K with and

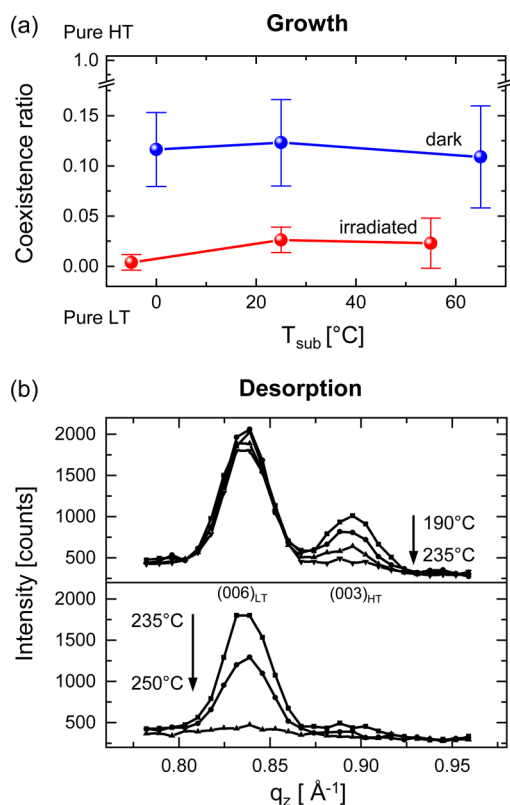


Figure 4. (a) Growth and nucleation of the HT phase in a temperature range of over 60 K, with and without laser illumination is suppressed more than a factor of 3–5 through illumination. (b) Desorption of 6T thin film in nitrogen atmosphere. Top: HT phase desorbs around 200 °C. Bottom: LT phase desorbs around 240 °C showing that in thin films the LT phase is more stable.

without laser illumination by calculating the phase coexistence ratio based on the integrated Bragg intensity of the $(003)_{\text{HT}}$ and $(600)_{\text{LT}}$ reflections. We find that this ratio between the two phases is independent of the substrate temperature T_{sub} within the range of 60 K. From this we conclude that possible substrate temperature changes within ± 5 °C due to the laser illumination can be neglected in comparison with the 60 K range in which the effect is observed.

In a further experiment the temperature dependence of desorption of the two polymorphs at elevated temperatures was studied to determine which of the two phases is more stable. To do so, we heated a previously grown 6T film on KCl step by step in a nitrogen atmosphere. X-ray scans at different temperatures allowed us to monitor and separate the temperatures at which the reflections of the two crystal phases disappear. The results are shown in Figure 4b. The reflections corresponding to the HT structure start to disappear at a

significantly lower temperature (190 °C) than the reflections of the LT structure (235 °C, both for flat lying and upright standing molecules). The lower thermal stability of the HT phase in our samples is an important factor in explaining why the HT phase is suppressed by light.

A further contribution to the suppression of the HT phase could be differing optical absorption of the two phases. In order to better understand whether the two phases absorb 532 nm light differently, e.g., through different absorption coefficients or spectral shifts, we performed ab initio calculations of the optical absorption spectra of HT and LT, in the framework of MBPT. The results are shown in Figure 5. We computed the

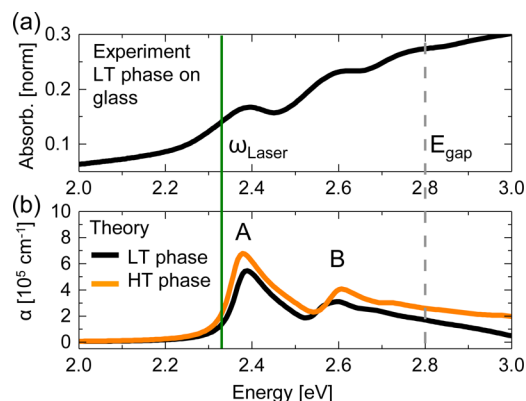


Figure 5. (a) Onset of the experimental LT absorption spectra close to the photoexcitation energy; (b) BSE calculation of the absorption coefficient α for an electric field lying on the substrate surface plane of LT and HT. The solid green line indicates the laser frequency ω_{Laser} (2.33 eV), while the gray dashed line at 2.8 eV is the computed fundamental gap for both structures. The peaks A and B are bound excitons. A Lorentzian broadening of 25 meV is applied to the computed spectra.

absorption coefficient α at normal incidence, with the electric field parallel to the substrate contact planes of the unit cells (b – c plane for LT and a – b plane for HT structure; see also Figure 1a). The computed peak positions of the LT polymorph agree with the experiment (see Figure 5). The HT spectrum is only theoretically accessible, as no pure HT films could be grown. Comparing the theoretical HT and LT spectra, we find that the two phases have very similar optical absorption. The low-energy part is characterized by two strong excitonic peaks, A and B, which lie within the gap, $E_g = 2.8$ eV, for both HT and LT. The binding energies of these excitons are E_b (A) = 0.41 eV and E_b (B) = 0.19 eV in the LT phase and E_b (A) = 0.45 eV and E_b (B) = 0.22 eV in HT. It is important to note that exciton A lies within 10 meV above the frequency of the green laser.

The similarity of the absorption energies of A and B in the two phases points toward a minor role of excitonic shifts in the selective growth of LT upon laser illumination. Although a slight difference in the absorbance can be observed in the spectra of Figure 5b, the height of peak A is about 20% smaller in LT compared to HT. This feature can be associated with the different orientation of the molecules on the substrate, as shown in Figure 1a. Since the optical transition giving rise to peak A is aligned along the long molecular axis, the HT phase with a lower tilt angle has a better alignment between the optical transition and the electric field direction of the laser leading to higher absorption.

DISCUSSION

The results presented above clearly indicate a direct influence of light on the crystallization behavior of 6T thin films beyond simple substrate heating. In the following we examine possible mechanisms that can explain this effect. These are excited-state crystallization, optical absorption with subsequent local heating of LT and HT nuclei, as well as different cohesive energies.

Crystallization in the photoexcited state has a negligible effect in this system, because the molecules are mostly in their ground state. Taking into account an absorption length of $\alpha = 93$ nm for 6T thin films⁴⁰ at 530 nm, there are roughly 10^5 absorbed photons per molecule for the given illumination at 1.5 W/cm² during the ~ 20 min growth time of one molecular monolayer. Because of the short excited-state lifetimes of less than $1 \mu\text{s}$ ⁴¹ combined with the low laser intensities, molecules are 99.999% of the time in the ground state under the assumption of similar luminescence behavior of the two phases.

As shown by first-principles calculations, the excitonic peak A, which is the closest to the wavelength of the illuminating laser, lies approximately at the same energy for the two phases. Hence, the influence of light on the growth of 6T cannot be explained by dissimilar absorption energies of peak A and thus a different overlap with the laser line. However, we notice that the oscillator strength in HT is 20% higher than in LT phase, due to the tilt of the molecules in the unit cell. Hence, molecules in the HT phase absorb more light than in the LT phase. Therefore, molecules in HT orientation exhibit an increased laser-induced heating and gain additional energy.

From the desorption behavior, we find a reduced thermal stability of the HT compared to the LT phase for the given sample morphology and phase mixture. The observed earlier desorption of the HT phase as compared to the LT phase seemingly contradicts results from bulk crystals, for which Della Valle et al. have found that the HT structure ($E_{\text{b HT}} = -247.38$ kJ/mol) is more stable than LT ($E_{\text{b LT}} = -245.94$ kJ/mol).²⁵ Preliminary first-principles calculations that we are currently carrying out confirm this trend. Similar results were obtained experimentally for the related molecule 4T by Campione et al., who measured 0.42 kJ/mol for the LT/HT crystal to crystal transition for 4T in single crystals.⁴² However, our finding of a higher stability of LT thin films can potentially be rationalized by taking into account surface energies, which play an important role in thin films with a large surface to volume ratio. It is often observed that in thin films more upright standing molecules are stabilized at the interface, and such surface induced phases have been observed for pentacene (PEN), diindenoperylene (DIP), and 4T.^{3,43,44} The experimental observation of higher stability of LT thin films when compared to HT thin films therefore could be due to lower surface energies of the LT phase with more upright molecules. Note that the thermodynamical stability of individual phases in general cannot purely be related to the desorption temperature, but is for example also influenced by desorption kinetics,^{45–47} island size and shape of the individual crystal grains in the respective phase.⁴⁸ Thus, the reduced desorption temperature of the HT phase compared to the LT phase may not apply to single crystals in the two phases and could also be specific to the analyzed thin film structure.

In conclusion, the combination of the lower thermal stability of the HT phase in thin films with stronger optical heating of molecules, as discussed above, can explain the origin of the observed phase purification. Additional contributions to the

complex growth kinetics and phase coexistence could come from nonthermal excitation of vibrational modes, photo-electronic charging, or an optical induced, direct phase transition from the HT into the LT phase. However, a quantification of these contributions goes beyond the scope of this work.

CONCLUSIONS

The crystallization of 6T and the phase purity in thin films can be influenced during growth by laser illumination of moderate intensity ($I = 1.5$ W/cm²). As a leading mechanism for this light-induced phase-purification, we suggest a combination of a slightly more intense optical absorption in the HT phase together with a lower thermal stability of the HT phase. This finding demonstrates that light can serve as an additional control parameter in molecular crystal growth to optimize the structural quality of molecular thin films. Eventually, micro-patterning may be considered as further application of this effect since light can be applied locally on the absorbing molecules.

ASSOCIATED CONTENT

Supporting Information

Additional information on coexisting LT phase crystallites with flat lying molecular orientation and a short description of the quantitative phase analysis as used in the Rietveld method. This material is available free of charge via the Internet at <http://pubs.acs.org>.

AUTHOR INFORMATION

Corresponding Author

*E-mail: stefan.kowarik@physik.hu-berlin.de.

Present Address

#ESRF - The European Synchrotron, 71 Avenue des Martyrs - CS 40220, 38043 Grenoble Cedex 9.

Notes

The authors declare no competing financial interest.

ACKNOWLEDGMENTS

This work was partially supported by DFG through SFB projects 951 and 658 and the Studienstiftung des Deutschen Volkes. We acknowledge the Paul Scherrer Institut, Villigen, Switzerland, for provision of synchrotron radiation beamtime at the MS beamline of the SLS and would like to thank P. Willmott for assistance. Furthermore, the authors thank Andreas Opitz and Kilian Wimmer for the helpful discussions. We thank J. P. Rabe for access to AFM instruments.

REFERENCES

- (1) Anthony, J. E. *Nat. Mater.* **2014**, *13*, 773–775.
- (2) Diao, Y.; Tee, B. C.-K.; Giri, G.; Xu, J.; Kim, D. H.; Becerril, H. a.; Stoltenberg, R. M.; Lee, T. H.; Xue, G.; Mannsfeld, S. C. B.; Bao, Z. *Nat. Mater.* **2013**, *12*, 665–671.
- (3) Mayer, A.; Kazimirov, A.; Malliaras, G. *Phys. Rev. Lett.* **2006**, *97*, 105503.
- (4) Iannotta, S.; Toccoli, T. J. *Polym. Sci., Part B: Polym. Phys.* **2003**, *41*, 2501–2521.
- (5) Simbrunner, C.; Nabok, D.; Hernandez-Sosa, G.; Oehzelt, M.; Djuric, T.; Resel, R.; Romaner, L.; Puschnig, P.; Ambrosch-Draxl, C.; Salzmann, I.; Schwabegger, G.; Watzinger, I.; Sitter, H. *J. Am. Chem. Soc.* **2011**, *133*, 3056–3062.

- (6) Beyer, P.; Breuer, T.; Ndiaye, S.; Zykov, A.; Viertel, A.; Gensler, M.; Rabe, J. P.; Hecht, S.; Witte, G.; Kowarik, S. *ACS Appl. Mater. Interfaces* **2014**, *6*, 21484–21493.
- (7) Yamamoto, Y.; Ichikawa, H.; Ueno, K.; Koma, a.; Saiki, K.; Shimada, T. *Phys. Rev. B* **2004**, *70*, 155415.
- (8) Sander, A.; Hammer, R.; Duncker, K.; Förster, S.; Widdra, W. *J. Chem. Phys.* **2014**, *141*, 104704.
- (9) Sugi, K.; Ishii, H.; Kimura, Y.; Niwano, M.; Ito, E.; Washizu, Y.; Hayashi, N.; Ouchi, Y.; Seki, K. *Thin Solid Films* **2004**, *464–465*, 412–415.
- (10) Balzer, F.; Rubahn, H.-G. *Nano Lett.* **2002**, *2*, 747–750.
- (11) Chen, L.; Cherniavskaya, O.; Shalek, A.; Brus, L. E. *Nano Lett.* **2005**, *5*, 2241–2245.
- (12) Ichikawa, H.; Saiki, K.; Suzuki, T.; Hasegawa, T.; Shimada, T. *Jpn. J. Appl. Phys.* **2005**, *44*, L1469–L1471.
- (13) Fichou, D. *J. Mater. Chem.* **2000**, *10*, 571–588.
- (14) Hörmann, U.; Wagner, J.; Gruber, M.; Opitz, A.; Brütting, W. *Phys. Status Solidi* **2011**, *5*, 241–243.
- (15) Opitz, A.; Wagner, J.; Brütting, W.; Salzmann, I.; Koch, N.; Manara, J.; Pflaum, J.; Hinderhofer, A.; Schreiber, F. *IEEE J. Sel. Top. Quantum Electron.* **2010**, *16*, 1707–1717.
- (16) LT structure: $a = 44.71 \text{ \AA}$, $b = 7.85 \text{ \AA}$, $c = 6.03 \text{ \AA}$; $\beta = 90.8^\circ$.
- (17) HT structure: $a = 9.14 \text{ \AA}$, $b = 5.68 \text{ \AA}$, $c = 20.67 \text{ \AA}$; $\beta = 97.78^\circ$.
- (18) Siegrist, T.; Fleming, R. M.; Haddon, R. C.; Laudise, R. A.; Lovinger, A. J.; Katz, H. E.; Bridenbaugh, P.; Davis, D. D. *J. Mater. Res.* **1995**, *10*, 2170–2173.
- (19) Lorch, C.; Banerjee, R.; Frank, C.; Dieterle, J.; Hinderhofer, A.; Gerlach, A.; Schreiber, F. *J. Phys. Chem. C* **2015**, *119*, 819–825.
- (20) Umbach, E.; Gebauer, W.; Soukopp, A.; Bässler, M.; Sokolowski, M. *J. Lumin.* **1998**, *76–77*, 641–651.
- (21) Garnier, F. *Curr. Opin. Solid State Mater. Sci.* **1997**, *2*, 455–461.
- (22) Servet, B.; Horowitz, G.; Ries, S.; Lagorsse, O.; Alnot, P.; Yassar, A.; Deloffre, F.; Srivastava, P.; Hajlaoui, R. *Chem. Mater.* **1994**, *6*, 1809–1815.
- (23) Lovinger, A. J.; Davis, D. D.; Ruel, R.; Torsi, L.; Dodabalapur, A.; Katz, H. E. *J. Mater. Res.* **1995**, *10*, 2958–2962.
- (24) Vogel, J.-O.; Salzmann, I.; Opitz, R.; Duhm, S.; Nickel, B.; Rabe, J. P.; Koch, N. *J. Phys. Chem. B* **2007**, *111*, 14097–14101.
- (25) Della Valle, R. G.; Venuti, E.; Brillante, A.; Girlando, A. *J. Phys. Chem. A* **2008**, *112*, 6715–6722.
- (26) Trabattoni, S.; Moret, M.; Campione, M.; Raimondo, L.; Sassella, A. *Cryst. Growth Des.* **2013**, *13*, 4268–4278.
- (27) Schwabegger, G.; Djuric, T.; Sitter, H.; Resel, R.; Simbrunner, C. *Cryst. Growth Des.* **2013**, *13*, 536–542.
- (28) Simbrunner, C. *Semicond. Sci. Technol.* **2013**, *28*, 053001.
- (29) Loi, M. A.; Como, E.; Da Dinelli, F.; Murgia, M.; Zamboni, R.; Biscarini, F.; Muccini, M. *Nat. Mater.* **2004**, *4*, 81–85.
- (30) Da Como, E.; Loi, M. A.; Murgia, M.; Zamboni, R.; Muccini, M. *J. Am. Chem. Soc.* **2006**, *128*, 4277–4281.
- (31) Willmott, P. R.; Meister, D.; Leake, S. J.; Lange, M.; Bergamaschi, A.; Böge, M.; Calvi, M.; Cancellieri, C.; Casati, N.; Cervellino, A.; Chen, Q.; David, C.; Flechsig, U.; Gozzo, F.; Henrich, B.; Jäggi-Spielmann, S.; Jakob, B.; Kalichava, I.; Karvinen, P.; Krempasky, J.; Lüdeke, A.; Lüscher, R.; Maag, S.; Quitmann, C.; Reinle-Schmitt, M. L.; Schmidt, T.; Schmitt, B.; Streun, A.; Vartiainen, I.; Vitins, M.; Wang, X.; Wullschleger, R. *J. Synchrotron Radiat.* **2013**, *20*, 667–682.
- (32) Gulans, A.; Kontur, S.; Meisenbichler, C.; Nabok, D.; Pavone, P.; Rigamonti, S.; Sagmeister, S.; Werner, U.; Draxl, C. *J. Phys.: Condens. Matter* **2014**, *26*, 363202.
- (33) Strinati, G. *La Riv. del Nuovo Cim.* **1988**, *11*, 1–86.
- (34) Sagmeister, S.; Ambrosch-Draxl, C. *Phys. Chem. Chem. Phys.* **2009**, *11*, 4451–4457.
- (35) Perdew, J. P.; Wang, Y. *Phys. Rev. B* **1992**, *45*, 13244–13249.
- (36) Horowitz, G.; Bachet, B.; Yassar, A.; Lang, P.; Demanze, F.; Fave, J.; Garnier, F. *Chem. Mater.* **1995**, *7*, 1337–1341.
- (37) Hill, R. J.; Howard, C. J. *J. Appl. Crystallogr.* **1987**, *20*, 467–474.
- (38) Langford, J. I.; Louër, D. *Rep. Prog. Phys.* **1996**, *59*, 131–234.
- (39) Soyer, A. *J. Appl. Crystallogr.* **1995**, *28*, 244–244.
- (40) Fichou, D.; Horowitz, G.; Xu, B.; Garnier, F. *Synth. Met.* **1992**, *48*, 167–179.
- (41) Cheng, X.; Ichimura, K.; Fichou, D.; Kobayashi, T. *Chem. Phys. Lett.* **1991**, *185*, 286–291.
- (42) Campione, M.; Tavazzi, S.; Moret, M.; Porzio, W. *J. Appl. Phys.* **2007**, *101*, 083512.
- (43) Frank, C.; Novák, J.; Banerjee, R.; Gerlach, A.; Schreiber, F.; Vorobiev, A.; Kowarik, S. *Phys. Rev. B* **2014**, *90*, 045410.
- (44) Campione, M.; Borghesi, A.; Laicini, M.; Sassella, A.; Goletti, C.; Bussetti, G.; Chiaradia, P. *J. Chem. Phys.* **2007**, *127*, 244703.
- (45) Käfer, D.; Wöll, C.; Witte, G. *Appl. Phys. A: Mater. Sci. Process.* **2008**, *95*, 273–284.
- (46) Moser, A.; Novák, J.; Flesch, H.-G.; Djuric, T.; Werzer, O.; Haase, A.; Resel, R. *Appl. Phys. Lett.* **2011**, *99*, 221911.
- (47) Yang, C. C.; Li, S.; Armellin, J. *J. Phys. Chem. C* **2007**, *111*, 17512–17515.
- (48) Kakudate, T.; Yoshimoto, N.; Saito, Y. *Appl. Phys. Lett.* **2007**, *90*, 081903.